



# Factors controlling temporal variability of near-ground atmospheric $^{222}\text{Rn}$ concentration over central Europe

M. Zimnoch<sup>1</sup>, P. Wach<sup>1</sup>, L. Chmura<sup>1,2</sup>, Z. Gorczyca<sup>1</sup>, K. Rozanski<sup>1</sup>, J. Godłowska<sup>2</sup>, J. Mazur<sup>3</sup>, K. Kozak<sup>3</sup>, and A. Jeričević<sup>4</sup>

<sup>1</sup>AGH University of Science and Technology, Faculty of Physics and Applied Computer Science, Krakow, Poland

<sup>2</sup>Institute of Meteorology and Water Management, National Research Institute, Krakow Branch, Krakow, Poland

<sup>3</sup>The Henryk Niewodniczanski Institute of Nuclear Physics, Polish Academy of Sciences, Krakow, Poland

<sup>4</sup>Croatian Civil Aviation Agency, Zagreb, Croatia

Correspondence to: M. Zimnoch (zimnoch@agh.edu.pl)

Received: 4 December 2013 – Published in Atmos. Chem. Phys. Discuss.: 10 February 2014

Revised: 18 July 2014 – Accepted: 28 July 2014 – Published: 16 September 2014

**Abstract.** Concentration of radon ( $^{222}\text{Rn}$ ) in the near-ground atmosphere has been measured quasi-continuously from January 2005 to December 2009 at two continental sites in Europe: Heidelberg (south-west Germany) and Krakow (southern Poland). The atmosphere was sampled at ca. 30 and 20 m above the local ground. Both stations were equipped with identical instruments. Regular observations of  $^{222}\text{Rn}$  were supplemented by measurements of surface fluxes of this gas in the Krakow urban area, using two different approaches. The measured concentrations of  $^{222}\text{Rn}$  varied at both sites in a wide range, from less than  $2.0\text{ Bq m}^{-3}$  to approximately  $40\text{ Bq m}^{-3}$  in Krakow and  $35\text{ Bq m}^{-3}$  in Heidelberg. The mean  $^{222}\text{Rn}$  content in Krakow, when averaged over the entire observation period, was 30% higher than in Heidelberg ( $5.86 \pm 0.09$  and  $4.50 \pm 0.07\text{ Bq m}^{-3}$ , respectively). Distinct seasonality of  $^{222}\text{Rn}$  signal is visible in the obtained time series of  $^{222}\text{Rn}$  concentration, with higher values recorded generally during late summer and autumn. The surface  $^{222}\text{Rn}$  fluxes measured in Krakow also revealed a distinct seasonality, with broad maximum observed during summer and early autumn and minimum during the winter. When averaged over a 5-year observation period, the night-time surface  $^{222}\text{Rn}$  flux was equal to  $46.8 \pm 2.4\text{ Bq m}^{-2}\text{ h}^{-1}$ . Although the atmospheric  $^{222}\text{Rn}$  levels at Heidelberg and Krakow appeared to be controlled primarily by local factors, it was possible to evaluate the “continental effect” in atmospheric  $^{222}\text{Rn}$  content between both sites, related to gradual build-up of  $^{222}\text{Rn}$  concentration in the air masses travelling between Heidelberg and Krakow. The mean value of this build-up was equal

to  $0.78 \pm 0.12\text{ Bq m}^{-3}$ . The measured minimum  $^{222}\text{Rn}$  concentrations at both sites and the difference between them was interpreted in the framework of a simple box model coupled with HYSPLIT (Hybrid Single Particle Lagrangian Integrated Trajectory) analysis of air mass trajectories. The best fit of experimental data was obtained for the mean  $^{222}\text{Rn}$  flux over the European continent equal to  $52\text{ Bq m}^{-2}\text{ h}^{-1}$ , the mean transport velocity of the air masses within the convective mixed layer of the planetary boundary layer (PBL) on their route from the Atlantic coast to Heidelberg and Krakow equal to  $3.5\text{ m s}^{-1}$ , the mean rate constant of  $^{222}\text{Rn}$  removal across the top of the PBL equal to the  $^{222}\text{Rn}$  decay constant and the mean height of the convective mixed layer equal to 1600 m.

## 1 Introduction

Radon ( $^{222}\text{Rn}$ ) is an alpha-emitting radioactive inert gas with a half-life of 3.8 days. It is a product of the decay of  $^{226}\text{Ra}$  which belongs to  $^{238}\text{U}$ -decay series. Uranium ( $^{238}\text{U}$ ) and its decay product,  $^{226}\text{Ra}$ , are ubiquitous in the Earth's crust and in the soils. Radon is being released into the pore space of the soils and diffuses into the atmosphere, where it decays to lead  $^{210}\text{Pb}$  via a chain of intermediate decay products. Under specific conditions (heavy-rain events),  $^{222}\text{Rn}$  decay products sticking to aerosol particles can be washed out from the atmosphere, resulting in underestimation of the measured radon concentrations when the radon progeny method

is employed. The flux of  $^{222}\text{Rn}$  into the atmosphere is controlled by the source term ( $^{226}\text{Ra}$  content in the soil and its vertical distribution), by physical properties of the upper soil layer (mineral structure, porosity, water content) and to some extent by short-term variations of physical parameters characterizing the soil–atmosphere interface (mainly atmospheric temperature and pressure) (e.g. Greeman and Rose, 1996; Levin et al., 2003; Taguchi et al., 2011).

First measurements of atmospheric  $^{222}\text{Rn}$  were performed in the late 1920s (Wigand and Wenk, 1928). A recent summary by Zhang et al. (2011) identifies 41 stations worldwide where  $^{222}\text{Rn}$  was measured regularly for periods longer than 1 year (USA – 8; Europe – 19; Asia – 12; South America, Australia, Africa – 5; remote ocean and polar regions – 7). In Europe, the earliest data sets originate from Paris (1955–1960) and Saclay (1956–1960) (Servant and Tanaevsky, 1961). Two major categories of  $^{222}\text{Rn}$  detection techniques have been employed in those studies: (i) various designs of ionization chambers measuring directly the alpha particles of  $^{222}\text{Rn}$ , and (ii) indirect methods based on measurements of radon decay products.

Due to a lack of important sinks apart from radioactive decay,  $^{222}\text{Rn}$  is an excellent tracer for atmospheric processes. Nowadays, major applications of radon in atmospheric research include (i) tracing of horizontal air mass transport (e.g. Dörr et al., 1983; Gerasopoulos et al., 2005); (ii) investigating vertical mixing in the lower atmosphere (Williams et al., 2008; Zahorowski et al., 2008, 2011); (iii) evaluation of atmospheric chemistry and transport models (e.g. Jacob et al., 1997; Chevillard et al., 2002; Gupta et al., 2004; Bergamaschi et al., 2006; Zhang et al., 2008); (iv) validation of the parameterisation schemes in numerical weather forecasting models (Jacob et al., 1997); and (v) assessing surface emissions of major greenhouse gases such as  $\text{CO}_2$ ,  $\text{N}_2\text{O}$  and  $\text{CH}_4$  (e.g. Schmidt et al., 1996, 2003; Levin et al., 1999, 2003; Biraud et al., 2000; Conen et al., 2002; van der Laan et al., 2009, 2010; Wilson et al., 1997).

Here we present an in-depth evaluation of two 5-year records of quasi-continuous near-ground atmospheric  $^{222}\text{Rn}$  concentration measurements performed at two continental sites in Europe: Heidelberg (south-west Germany) and Krakow (southern Poland). The records were obtained using identical instruments located in similar settings (urban environment). The primary objective of our work was the identification of major factors controlling temporal variability of atmospheric  $^{222}\text{Rn}$  concentration observed at the both sites at diurnal, synoptic and seasonal timescales. This included, among others, the measurements of local surface fluxes of this gas in the Krakow urban area using two different approaches. The second objective of the study was linked with the specific location of the two  $^{222}\text{Rn}$  monitoring sites (similar latitudinal position with different distance to the Atlantic coast, along a major pathway of air mass transport across Europe). It was aimed at quantification of the “continental effect” associated with build-up of  $^{222}\text{Rn}$  in the atmosphere

over the European continent and its interpretation in the framework of a simple model.

## 2 Measurement sites

The measurement sites are located at the same latitudinal band (ca.  $50^\circ\text{N}$ ), in a similar urban setting, with the distance to the Atlantic Ocean equal to approximately 600 km for Heidelberg and 1600 km for Krakow. Both measurement sites were equipped with identical instruments (Levin et al., 2002), and the atmosphere was sampled at a comparable level. The meteorological parameters (wind speed, wind direction and temperature) were monitored at the same elevation at which the inlet systems of the instruments measuring radon concentration were installed.

Krakow (approx. 800 000 inhabitants) is located in southern Poland. Characteristic features of the local climate are generally weak winds and frequent atmospheric temperature inversion situations, sometimes extending over several days. The average wind speed calculated for the period 2005–2007 was  $1.9\text{ m s}^{-1}$ . West and south-west directions of surface winds prevail. Westerly circulation is generally connected with stronger winds (wind speeds above  $4\text{ m s}^{-1}$ ). Periods characterized by low wind speeds ( $< 1\text{ m s}^{-1}$ ), favouring accumulation of  $^{222}\text{Rn}$  in the near-ground atmosphere, constituted 34 % of the total time considered. Monthly mean air temperature at the site reveals a distinct seasonal cycle, with summer maximum (July–August) reaching  $19\text{--}24^\circ\text{C}$  and winter minimum (January–February) between  $-5$  and  $+2^\circ\text{C}$ . Monthly precipitation rates are more irregular, with a broad maximum during summer and minimum during winter months. The radon monitoring site ( $50^\circ 04'\text{N}$ ,  $19^\circ 55'\text{E}$ , 220 m a.s.l.) was located on the campus of the AGH University of Science and Technology, situated in the western sector of the city, bordering recreation and sports grounds. An air intake for  $^{222}\text{Rn}$  measurements was located on the roof of the Faculty of Physics and Applied Computer Science building, 20 m above the local ground. The site where surface fluxes of  $^{222}\text{Rn}$  were measured was located on the premises of the Institute of Nuclear Physics, Polish Academy of Sciences, situated in the western outskirts of the city, approximately 3 km north-west from the location of atmospheric  $^{222}\text{Rn}$  measurements. The soil type at the chamber location was Endogleyic Cambisol (IUSS, 2007), dominated by silty clay loam. The mean concentration of  $^{226}\text{Ra}$  in the soil profile, the precursor of  $^{222}\text{Rn}$ , was equal to  $22 \pm 3\text{ Bq kg}^{-1}$  (Mazur, 2008).

Heidelberg (approximately 130 000 inhabitants) is located in the upper Rhine Valley, in south-west Germany. Monthly mean surface air temperatures vary within the range  $1\text{--}3^\circ\text{C}$  during winter months and  $18\text{--}22^\circ\text{C}$  during the summer. The local atmospheric circulation patterns in Heidelberg are dominated by alternate north–south flow along the Rhine Valley, but also by frequent easterly winds from the Neckar Valley (Levin et al., 1999). The average wind speed calculated for

the period 2005–2007 was  $3.0 \text{ m s}^{-1}$  while low wind speed ( $< 1 \text{ m s}^{-1}$ ) periods constituted only 9.8 % of the total time considered. In contrast to local, near-surface wind direction, backward air trajectories calculated for the Heidelberg site clearly demonstrate predominance of westerly air masses. Air inlet for  $^{222}\text{Rn}$  measurements was installed on the roof of the Institute of Environmental Physics building ( $49^\circ 24' \text{ N}$ ,  $8^\circ 42' \text{ E}$ ,  $116 \text{ m a.s.l.}$ ),  $30 \text{ m}$  above the local ground.

### 3 Methods

#### 3.1 Measurements of $^{222}\text{Rn}$ content in the near-ground atmosphere

Regular measurements of  $^{222}\text{Rn}$  content in the near-ground atmosphere were performed with the aid of a radon monitor. The instrument was developed at the Institute of Environmental Physics, University of Heidelberg, Germany (Levin et al., 2002), and made available for this study. The instrument measures specific activity of  $^{222}\text{Rn}$  in air through its daughter products. The air is pumped with the constant flow rate through a glass filter (Whatman QM-A,  $2.2 \mu\text{m}$ ) which is placed directly over the surface-barrier detector measuring alpha particles emitted by  $^{222}\text{Rn}$  and  $^{220}\text{Rn}$  daughter products deposited on the filter. The instrument records alpha decay energy spectra accumulating in  $30 \text{ min}$  counting intervals. The spectra contain peaks representing decay products of  $^{222}\text{Rn}$  ( $^{214}\text{Po}$ ,  $E_\alpha = 7.7 \text{ MeV}$ ;  $^{218}\text{Po}$ ,  $E_\alpha = 6 \text{ MeV}$ ) as well as  $^{220}\text{Rn}$  ( $^{212}\text{Po}$ ,  $E_\alpha = 8.8 \text{ MeV}$ ;  $^{212}\text{Bi}$ ,  $E_\alpha = 6.1 \text{ MeV}$ ). By energy discrimination and a dedicated data evaluation protocol taking into account disequilibrium between daughter products of  $^{222}\text{Rn}$  at the end of each counting interval, as well as empirically determined disequilibrium between  $^{222}\text{Rn}$  gas and its daughter products in the atmosphere, the specific activity of the  $^{222}\text{Rn}$  gas in air can be calculated. The mean disequilibrium has been determined by parallel measurements of atmospheric  $^{222}\text{Rn}$  activity with an absolutely calibrated slow-pulse ionization chamber and the radon monitor to  $1/1.367$ , for the elevation of  $20 \text{ m}$  above the local ground in Heidelberg (Levin et al., 2002).

#### 3.2 Measurements of surface $^{222}\text{Rn}$ fluxes in Krakow

Two different approaches were used to quantify the magnitude and temporal variability of surface fluxes of  $^{222}\text{Rn}$  into the local atmosphere: (i) night-time  $^{222}\text{Rn}$  fluxes were derived from measurements of atmospheric  $^{222}\text{Rn}$  content near the ground, combined with quasi-continuous measurements of the mixing layer height within the planetary boundary layer (PBL) and modelling of vertical  $^{222}\text{Rn}$  profiles in the atmosphere using a regional transport model and (ii) point measurements of soil  $^{222}\text{Rn}$  fluxes were performed using a specially designed exhalation chamber system connected to an AlphaGUARD radon detector.

#### 3.2.1 Sodar-assisted estimates of night-time $^{222}\text{Rn}$ fluxes

##### Theory

During the day, with active vertical convection of air in the lower atmosphere, radon emitted from the soil is diluted in a large volume of mixing layer within the PBL, leading to relatively low  $^{222}\text{Rn}$  concentrations observed close to the ground. During late afternoon, when the vertical gradient of air temperature changes the sign, drastic reduction of vertical mixing occurs. This process leads to accumulation of  $^{222}\text{Rn}$  in the near-ground atmosphere during the night. The rate of nocturnal increase of  $^{222}\text{Rn}$  concentration is controlled by the mixing layer height according to the mass balance equation

$$H \frac{dC_m}{dt} = F_{\text{in}} - F_{\text{out}}, \quad (1)$$

where  $H$  is the height of the mixing layer,  $C_m$  is the mean concentration of  $^{222}\text{Rn}$  within the mixing layer,  $F_{\text{in}}$  is surface flux of  $^{222}\text{Rn}$  and  $F_{\text{out}}$  is the flux of  $^{222}\text{Rn}$  associated with removal processes (horizontal and vertical transport, radioactive decay). For nights with low wind speed ( $< 1 \text{ m s}^{-1}$ ) and the adopted frequency of measurements, this term can be neglected.

During stable atmospheric conditions with low wind speeds, a distinct vertical gradient of  $^{222}\text{Rn}$  concentration is established within the PBL. As the measurements of  $^{222}\text{Rn}$  content are performed close to the surface, at the height of approximately  $20 \text{ m}$ , a correction factor  $k$  relating the increase of the mean  $^{222}\text{Rn}$  concentration within the mixing layer ( $dC_m/dt$ ) to the increase of  $^{222}\text{Rn}$  concentration observed close to the ground ( $dC_{\text{surf}}/dt$ ) should be introduced to Eq. (1):

$$F_{\text{in}} = \frac{H}{k} \frac{dC_{\text{surf}}}{dt}, \quad (2)$$

where  $H$  is the mixing layer height,  $k$  is the correction factor and  $C_{\text{surf}}$  is the concentration of  $^{222}\text{Rn}$  at the adopted measurement height.

##### Modelling

The correction factor  $k$  was quantified using vertical profiles of  $^{222}\text{Rn}$  simulated by the European Monitoring and Evaluation Programme (EMEP) model. The Unified EMEP model (<http://www.emep.int/>) was developed at the Norwegian Meteorological Institute under EMEP. In this work, the Unified EMEP model version rv2\_6\_1 was used. The model is fully documented in Simpson et al. (2012). It simulates the atmospheric transport and deposition of various trace compounds, as well as photo-oxidants and particulate matter over Europe. The Unified EMEP model uses 3-hourly meteorological data from the PARAllel Limited Area Model with the Polar Stereographic map projection (PARLAM-PS), which is a dedicated version of the High Resolution Limited Area Model

(HIRLAM) for use within EMEP. The model has been extensively validated against measurements (e.g. Jeričević et al., 2010). In the framework of the presented study, the model was adopted to calculate regional transport of  $^{222}\text{Rn}$ . The model domain (Fig. 1S in the Supplement) covers Europe and the Atlantic Ocean with the grid size of  $50\text{ km} \times 50\text{ km}$  and 20 layers in vertical, reaching up to 100 hPa.

The Unified EMEP model was used to simulate vertical profiles of  $^{222}\text{Rn}$  concentrations in the atmosphere for the location of Krakow for 1 full year (2005) with hourly time resolution, assuming spatially constant exhalation rate of  $1\text{ atom cm}^{-2}\text{ s}^{-1}$  over the continent. Model results corresponding to the periods starting at sunset and ending 6 h later for each night were used. The  $^{222}\text{Rn}$  concentration at the measurement height (20 m above the ground) was evaluated from the simulated profiles using exponential fit to the model data. The mean radon concentration in the mixing layer was calculated as the mean  $^{222}\text{Rn}$  content in the lowest five layers of the model, representing approximately the first 600 m of the troposphere, weighted by the thickness of the corresponding layers:

$$C_m = \frac{\sum_{i=1}^5 C_i h_i}{\sum_{i=1}^5 h_i}, \quad (3)$$

where  $C_m$  is the modelled mean concentration of  $^{222}\text{Rn}$  within the mixing layer,  $C_i$  is the mean  $^{222}\text{Rn}$  concentration in the layer  $i$  (model data) and  $h_i$  is thickness of the layer  $i$ .

In the next step, the growth rates of the mean  $^{222}\text{Rn}$  concentration within the mixing layer ( $\Delta C_m$ ) and at 20 m above the ground ( $\Delta C_{\text{surf}}$ ) were calculated for each considered period using linear regression fit to the data. Finally, the  $k$  factor was calculated for each night:

$$k = \frac{\Delta C_{\text{surf}}}{\Delta C_m}. \quad (4)$$

The monthly mean  $k$  values were calculated using the values of this parameter assigned for each night, after a two-step selection procedure. In the first step, only the periods characterized by well-defined growth rates  $\Delta C_m$  and  $\Delta C_{\text{surf}}$  ( $R^2 > 0.8$ ) were selected. In the second step, periods characterized by high wind speeds within the first layer of the model ( $v > 3\text{ m s}^{-1}$ ) were removed. The monthly mean  $k$  values calculated using the above-outlined procedure are presented together with their uncertainties in Fig. 2S in the Supplement. The  $k$  value for January 2005 is missing because no single night in this month fulfilled the adopted selection criteria. Since model results were available only for 2005, the monthly mean  $k$  values presented in Fig. 2S in the Supplement were further smoothed using CCGvu 4.40 routine (Thoning et al., 1989). The smoothed curve (heavy line in Fig. 2S) was then used in calculations of surface fluxes of  $^{222}\text{Rn}$  (see subsection ‘‘Calculations of night-time  $^{222}\text{Rn}$  fluxes’’ of Sect. 3.2.1).

## Measurements of mixing height using sodar

The mixing layer height,  $H$ , was monitored using VDS sodar (Vertical Doppler Sodar, Version 3) built by the Krakow Branch of the Institute of Meteorology and Water Management. Detailed description of the sodar system can be found in Netzel et al. (1995) and Zimnoch et al. (2010). Sodar records were analysed manually. Stability of the surface layer was identified through unique features of sodar echoes, and its range was defined by determining the height of the observed structures at the upper level where mixing processes still exist (Piringer and Joffre, 2005). The sodar system was located inside a park complex, between the city centre and the industrial district, at the distance of ca. 6 km east from the location where atmospheric  $^{222}\text{Rn}$  measurements were performed. To examine possible influence of the distance between the sodar and  $^{222}\text{Rn}$  measurement sites on the calculated  $^{222}\text{Rn}$  fluxes, two dedicated measurement campaigns were performed. During the first campaign, lasting 1 month,  $^{222}\text{Rn}$  measurements were performed directly at the sodar site. Then, the sodar system was moved to the permanent location of the  $^{222}\text{Rn}$  monitoring system. During both campaigns neither significant change in the mixing layer height variability nor the range of calculated fluxes was observed (Zimnoch et al., 2010).

## Calculations of night-time $^{222}\text{Rn}$ fluxes

Each period considered in the calculations of night-time  $^{222}\text{Rn}$  fluxes started typically at sunset and ended 6 h later. Average height of the mixing layer was calculated from hourly sodar data for each analysed night. In building monthly mean night-time  $^{222}\text{Rn}$  fluxes, individual fluxes calculated for each night using Eq. (2) were subject to a two-step data selection algorithm. In the first step, only the nights for which the growth rate of the measured  $^{222}\text{Rn}$  concentration was well defined ( $R^2 > 0.8$ ) were selected. In the second step, the nights with the standard uncertainty of the mean mixing-layer height  $u(H)$  larger than 30 m, calculated from hourly values of this parameter derived from the sodar measurements, were removed from the remaining data set. For some months, the adopted data selection procedure resulted in significant reduction of the number of available data, leading to relatively large uncertainty of the corresponding monthly mean values of the calculated night-time  $^{222}\text{Rn}$  fluxes. The number of data used for calculation of the mean for each month varied between 5 and 23, with a mean value of 13. The first step of data selection reduced the amount of data by 34 %, and the second step by an additional 11 %. Sensitivity analysis showed that modification of  $R^2$  and  $u(H)$  values used in the data selection by 10 % results in reduction of the pool of data suitable for calculation of monthly means by 8 and 6 %, respectively.

### 3.2.2 Measurements of surface $^{222}\text{Rn}$ fluxes using the chamber method

The sodar-assisted assessment of surface night-time  $^{222}\text{Rn}$  fluxes in the Krakow agglomeration was supplemented by 1-year-long measurements of soil radon fluxes using the in-growth chamber method. The fluxes were measured using a specially designed, automatic exhalation chamber, connected with AlphaGUARD radon monitor (Mazur, 2008). The parameters of the chamber were as follows: (i) flow rate –  $0.3\text{ L min}^{-1}$ ; (ii) insertion depth – 6 cm; and (iii) diameter – 21.6 cm. The air trapped inside the chamber was circulated in a closed circuit for about 90 min, and the concentration of radon accumulated in the chamber was recorded every 10 min. The radon flux was determined from the slope of the straight line fitted to individual readings (Mazur, 2008; Vaupotič et al., 2010). A special device was constructed which enabled automatic movement of the exhalation chamber, down to the ground for radon flux measurement and up for ventilation of the system (Mazur, 2008). The  $^{222}\text{Rn}$  fluxes were measured up to eight times per day. Only night-time measurements (up to four in total) were used for comparison with sodar-assisted estimates of surface  $^{222}\text{Rn}$  flux representing night-time periods. The available raw data are presented in Fig. 3S in the Supplement.

## 4 Results and discussion

Time series of hourly mean concentrations of atmospheric  $^{222}\text{Rn}$  obtained at Heidelberg and Krakow between January 2005 and December 2009 are shown in Fig. 1. The gaps in time series of  $^{222}\text{Rn}$  content from June till December 2007 in Krakow and from June to July 2006 in Heidelberg were caused by technical problems with radon monitors. It is apparent from Fig. 1 that  $^{222}\text{Rn}$  content varies at both sites in a relatively wide range, from less than  $2\text{ Bq m}^{-3}$  to approximately  $40\text{ Bq m}^{-3}$  in Krakow and  $35\text{ Bq m}^{-3}$  in Heidelberg. The mean  $^{222}\text{Rn}$  concentration in Krakow averaged over the entire observation period ( $5.86 \pm 0.09\text{ Bq m}^{-3}$ ) is 30 % higher as compared to Heidelberg ( $4.50 \pm 0.07\text{ Bq m}^{-3}$  – cf. Table 1).

### 4.1 Diurnal changes of $^{222}\text{Rn}$ content in the near-ground atmosphere

Diurnal changes of  $^{222}\text{Rn}$  concentration in the near-ground atmosphere over Krakow and Heidelberg, averaged separately for each hour of the day over the entire observation period (January 2005–December 2009) and for each season (spring, summer, autumn, winter), are summarized in Fig. 2a and b. Irrespective of season, the measured  $^{222}\text{Rn}$  contents at both sites reveal characteristic behaviour, with elevated concentrations during night hours and reduced concentrations during midday. However, the shape and amplitude of daily

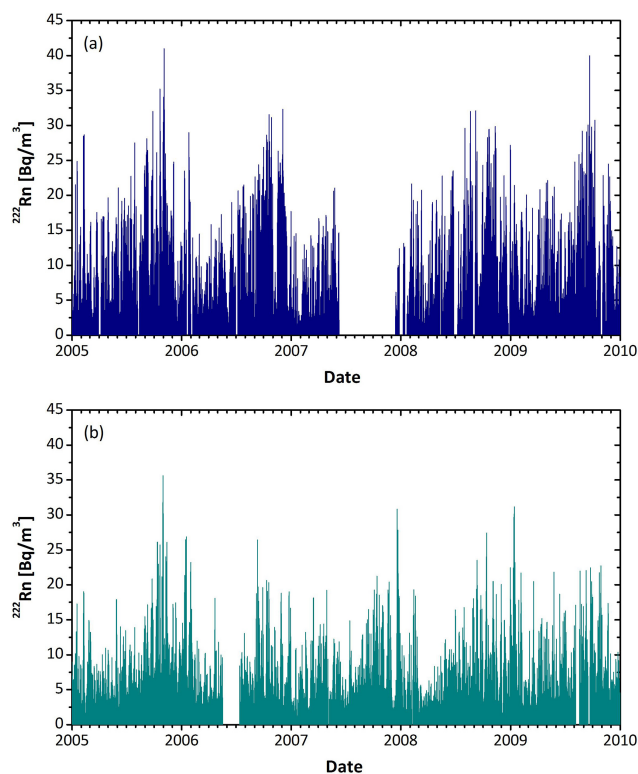


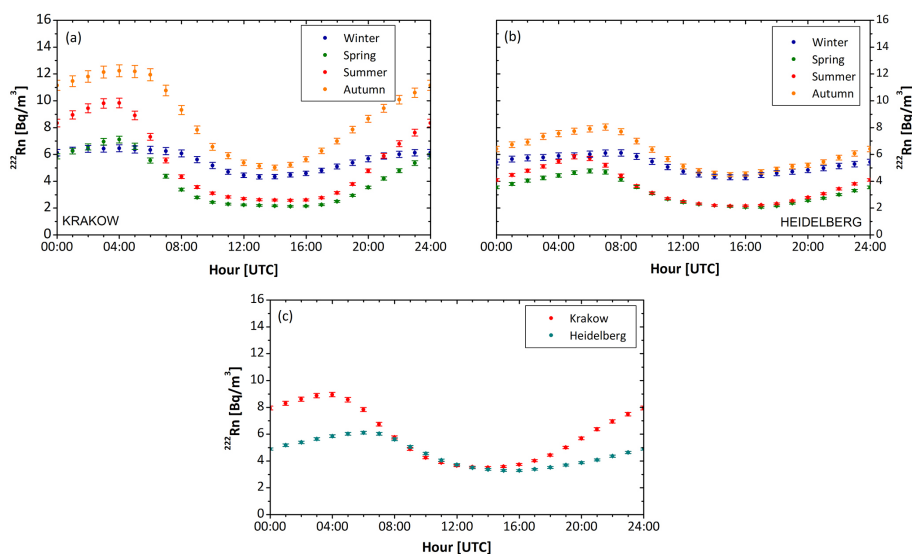
**Figure 1.** Time series of hourly mean  $^{222}\text{Rn}$  content in the near-ground atmosphere, recorded between January 2005 and December 2009 in Krakow, southern Poland (a), and Heidelberg, south-west Germany (b).

changes of  $^{222}\text{Rn}$  content vary significantly with the season and the observation site.

During winter months (December–February), daily variations of  $^{222}\text{Rn}$  are remarkably similar at both locations. The average  $^{222}\text{Rn}$  content for that period is equal to  $5.65 \pm 0.17\text{ Bq m}^{-3}$  at Krakow and  $5.19 \pm 0.19\text{ Bq m}^{-3}$  at Heidelberg, with peak-to-peak amplitude of diurnal changes reaching  $1.5\text{ Bq m}^{-3}$  at both sites (cf. Fig. 2 and Table 1). Daily minima are shallow and reduced in duration. During spring and summer months (March–May and June–August, respectively) the peak-to-peak amplitude of daily changes of  $^{222}\text{Rn}$  concentration increases significantly. This increase is particularly well pronounced in Krakow (the spring and summer amplitudes reach  $4.7$  and  $7.0\text{ Bq m}^{-3}$ , respectively) as compared to Heidelberg ( $2.5$  and  $3.5\text{ Bq m}^{-3}$ , respectively). At the same time, broader daily minima are observed at both sites, reflecting the growing role of vertical mixing within the PBL, driven by longer exposure of the surface to sunlight. The most pronounced differences between both sites are observed during autumn months (September–November). In Krakow, the maxima of atmospheric  $^{222}\text{Rn}$  content occur usually in the early-morning hours (ca. 4–6 a.m. UTC) and reach  $12\text{ Bq m}^{-3}$ , followed by a distinct minimum of  $5\text{ Bq m}^{-3}$  recorded usually between 13:00 and 14:00 UTC. In

**Table 1.** Indicators of daily variations of  $^{222}\text{Rn}$  activity in Krakow (KR) and Heidelberg (HD) during the period January 2005–December 2009. The quoted uncertainties represent standard uncertainties of the mean values.

Period		Mean daily $^{222}\text{Rn}$ activity ( $\text{Bq m}^{-3}$ )	Mean daily maximum $^{222}\text{Rn}$ activity ( $\text{Bq m}^{-3}$ )	Mean daily minimum $^{222}\text{Rn}$ activity ( $\text{Bq m}^{-3}$ )	Peak-to-peak amplitude ( $\text{Bq m}^{-3}$ )
Winter (Dec–Feb)	KR	$5.65 \pm 0.17$	$9.36 \pm 0.27$	$2.99 \pm 0.11$	$6.37 \pm 0.23$
	HD	$5.19 \pm 0.19$	$7.93 \pm 0.26$	$3.10 \pm 0.14$	$4.83 \pm 0.17$
Spring (Mar–May)	KR	$4.00 \pm 0.09$	$8.81 \pm 0.23$	$1.52 \pm 0.05$	$7.29 \pm 0.22$
	HD	$3.14 \pm 0.08$	$5.74 \pm 0.16$	$1.54 \pm 0.05$	$4.21 \pm 0.15$
Summer (Jun–Aug)	KR	$5.50 \pm 0.13$	$12.11 \pm 0.30$	$2.02 \pm 0.05$	$10.09 \pm 0.27$
	HD	$3.55 \pm 0.07$	$6.88 \pm 0.17$	$1.61 \pm 0.04$	$5.27 \pm 0.15$
Autumn (Sep–Nov)	KR	$8.70 \pm 0.23$	$15.59 \pm 0.39$	$3.83 \pm 0.13$	$11.76 \pm 0.35$
	HD	$6.08 \pm 0.17$	$10.13 \pm 0.27$	$3.38 \pm 0.13$	$6.75 \pm 0.21$
Mean (2005–2009)	KR	$5.86 \pm 0.09$	$11.28 \pm 0.16$	$2.55 \pm 0.05$	$8.72 \pm 0.14$
	HD	$4.50 \pm 0.07$	$7.67 \pm 0.12$	$2.42 \pm 0.05$	$5.26 \pm 0.09$

**Figure 2.** Diurnal variations of  $^{222}\text{Rn}$  concentration in the near-ground atmosphere over Krakow (a) and Heidelberg (b) during the period January 2005–December 2009, averaged separately for each hour and for four seasons: winter (DJF), spring (MAM), summer (JJA) and autumn (SON). Diurnal variation of  $^{222}\text{Rn}$  content at both sites averaged for the entire observation period is also shown (c). Vertical marks accompanying the data points indicate standard uncertainties of the calculated mean values.

Heidelberg, the early-morning maxima reach only  $8 \text{ Bq m}^{-3}$ , while the minima are maintained at approximately the same level as in Krakow (ca.  $5 \text{ Bq m}^{-3}$ ).

Diurnal variations of  $^{222}\text{Rn}$  content at both monitoring sites, averaged over the entire observation period, are shown in Fig. 2c. It is apparent that higher peak-to-peak amplitude of daily  $^{222}\text{Rn}$  variations in Krakow is primarily due to higher build-up of  $^{222}\text{Rn}$  during night hours at this site as compared to Heidelberg. The nocturnal build-up of radon in Krakow starts and ends approximately 2 h earlier as compared to Heidelberg (at ca. 15:00 and 04:00 UTC, respectively). This difference may partly stem from the fact that,

while both stations are located in the same time zone, the true solar time is shifted by approximately 1 h.

The source strength of  $^{222}\text{Rn}$  in the soil and the upward transport of this gas into the atmosphere does not vary significantly on an hourly timescale, except for frontal situations with fast changes of atmospheric pressure or during prolonged rainfall events. Therefore, diurnal variations of the concentration of this gas in the near-ground atmosphere presented in Fig. 2 primarily reflect the changes in stability of the lower troposphere and the resulting intensity of vertical mixing.

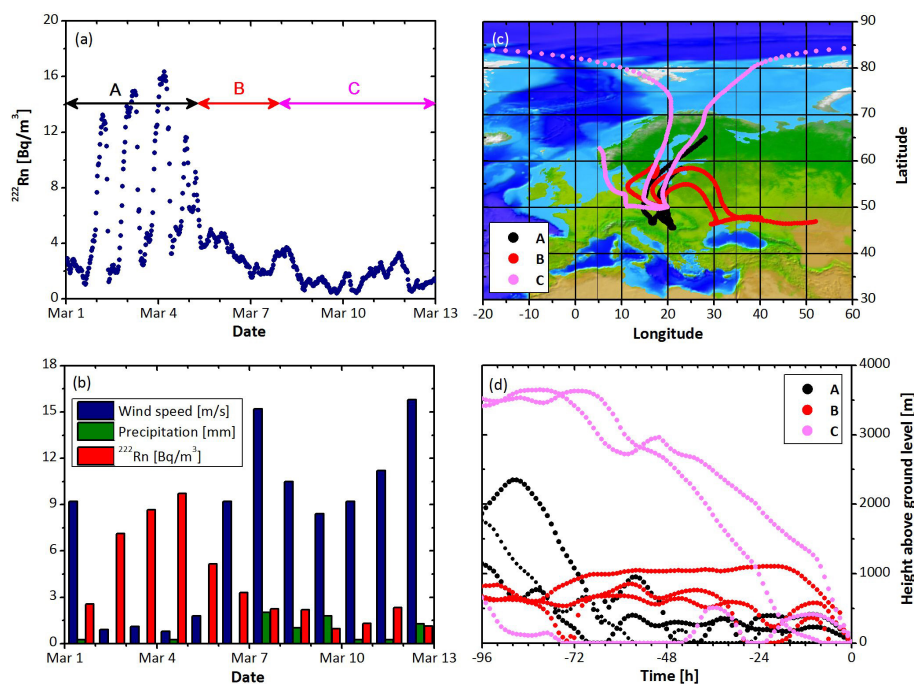


**Figure 3.** (a) Changes of atmospheric  $^{222}\text{Rn}$  concentration in Krakow between 1 and 13 March, 2005. Horizontal lines with arrows and letter symbols mark different air masses identified in (c). (b) Daily means of atmospheric  $^{222}\text{Rn}$  concentration, wind speed and rainfall amount in Krakow. (c) 96 h backward trajectories of the air masses arriving in Krakow, starting at 25, 50 and 75 % of the time period A, B and C marked in (a). (d) Changes of the elevation of trajectories shown in (c).

#### 4.2 Synoptic timescale changes of $^{222}\text{Rn}$ content in the near-ground atmosphere

While the amplitude of diurnal changes of  $^{222}\text{Rn}$  content is controlled primarily by the intensity of vertical mixing, its variations on a synoptic timescale (days to weeks) should be also a function of the origin of air masses passing through the given measurement site. One example illustrating the influence of synoptic-scale phenomena on the atmospheric  $^{222}\text{Rn}$  concentrations measured in Krakow is discussed below.

Temporal evolution of atmospheric  $^{222}\text{Rn}$  content in Krakow during the period from 1 to 13 March 2005 is shown in Fig. 3 in relation to wind speed, precipitation rates and 96 h backward trajectories of air masses passing the measurement location. Between 1 and 4 March, the measured  $^{222}\text{Rn}$  content revealed strong diurnal variations (Fig. 3a), with the maximum  $^{222}\text{Rn}$  concentrations reaching  $16 \text{ Bq m}^{-3}$ , superimposed on the growing trend of mean daily concentration of this gas (Fig. 3b). Air masses passing the sampling site during this period originated in north-central Europe (Fig. 3c). Very low wind speed facilitated gradual build-up of nighttime  $^{222}\text{Rn}$  in the local atmosphere during these days, as well as an increase of daytime background level caused by the increase in “continentality” of the air masses. From 5 March onwards, the course of atmospheric  $^{222}\text{Rn}$  content has changed radically; diurnal variations almost disappeared (Fig. 3a), while the average daily  $^{222}\text{Rn}$  content dropped

from  $9.7 \text{ Bq m}^{-3}$  for 4 March to  $5.2 \text{ Bq m}^{-3}$  for 5 March and  $3.3 \text{ Bq m}^{-3}$  for 6 March. This substantial change was clearly linked to change of circulation and sharp increase of wind speed (Fig. 3b, c). Between 5 and 7 March the sampling location was under the influence of air masses originating over Russia and Estonia, passing westward at relatively high elevation over the Baltic Sea and then turning south-east in the direction of Poland. Between 8 and 12 March the sampling location was under the influence of maritime air masses originating over the Arctic Sea and travelling southward at very high elevation with high speed. The rainfall occurring in Krakow during this period (between 0.5 and 2.0 mm) was associated with a frontal situation (drop of atmospheric pressure from 1000 hPa at 8 March to 965 hPa three days later). During the second part of this period, a small increase of  $^{222}\text{Rn}$  concentration correlated with significant reduction of the elevation of trajectories arriving in Krakow was observed.

The data shown in Fig. 3 clearly demonstrate a strong link between the measured  $^{222}\text{Rn}$  content in the near-ground continental atmosphere and weather-related phenomena such as history of air masses and wind speed. Concentrations of atmospheric  $^{222}\text{Rn}$  may change significantly on a synoptic timescale in response to these factors.

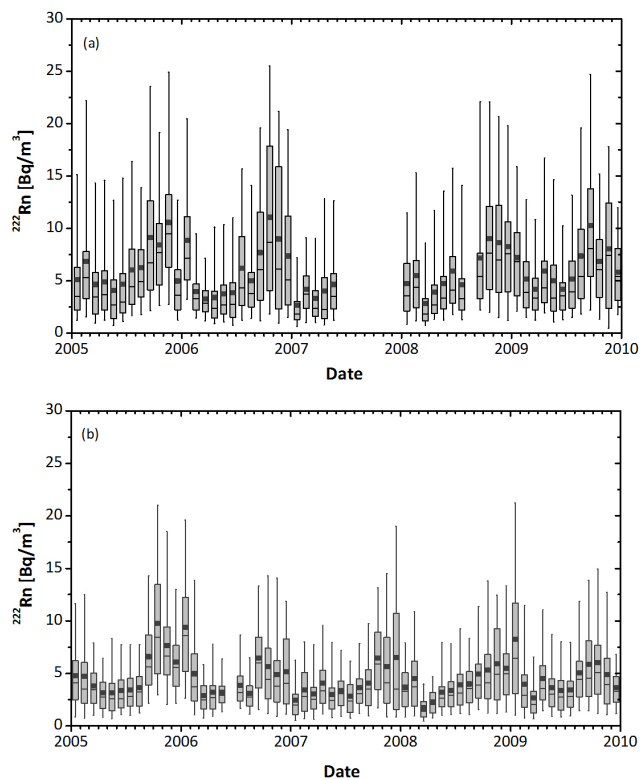


**Figure 4.** Box-and-whisker plot of monthly  $^{222}\text{Rn}$  concentration recorded in the near-ground atmosphere of Krakow (a) and Heidelberg (b) between January 2005 and December 2009. Marked percentiles represent the 5, 25, 75 and 95 % confidence interval; black squares represent medians; and horizontal lines represent mean values.

### 4.3 Seasonal variations of $^{222}\text{Rn}$ content in the near-ground atmosphere

Figure 4 shows monthly means of  $^{222}\text{Rn}$  content in the near-ground atmosphere, as observed in Krakow and Heidelberg between January 2005 and December 2009. The medians reveal a distinct seasonal trend, with a broad minimum of  $^{222}\text{Rn}$  content in spring and summer and maximum in autumn months. Monthly maxima are significantly higher in Krakow, reaching  $25 \text{ Bq m}^{-3}$ , compared to  $20 \text{ Bq m}^{-3}$  in Heidelberg. Monthly minima are comparable at both locations.

### 4.4 Surface fluxes of $^{222}\text{Rn}$ in Krakow

The monthly mean night-time fluxes of  $^{222}\text{Rn}$  in the Krakow urban area, derived from atmospheric  $^{222}\text{Rn}$  observations and sodar measurements of the mixing layer height using the methodology outlined in Sect. 3.2.1, are presented in Fig. 5. They cover the period June 2004–May 2009. Error bars indicate standard uncertainties of the monthly mean values. Blue bars represent the number of nights used for calculation of the monthly means. As seen in Fig. 5, high night-time

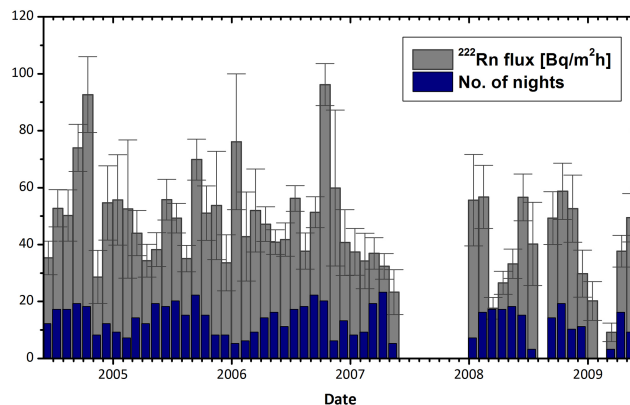


**Figure 5.** Monthly mean night-time fluxes of  $^{222}\text{Rn}$  in the Krakow urban area for the period June 2004–May 2009, derived from atmospheric  $^{222}\text{Rn}$  observations and sodar measurements of the mixing layer height (see text for details). Error bars indicate standard uncertainties of the mean values. Blue bars represent the number of nights used for calculation of the monthly means.

$^{222}\text{Rn}$  fluxes were obtained for autumn months (September, October, November) reaching  $80\text{--}90 \text{ Bq m}^{-2} \text{ h}^{-1}$ . When averaged over the entire observation period, the mean  $^{222}\text{Rn}$  night-time flux obtained for the Krakow urban area is equal to  $46.8 \pm 2.4 \text{ Bq m}^{-2} \text{ h}^{-1}$ . This value coincides with approximately  $46 \text{ Bq m}^{-2} \text{ h}^{-1}$ , derived for the location of Krakow from the map of  $^{222}\text{Rn}$  flux in Europe obtained from terrestrial  $\gamma$ -dose rate data (Szegvary et al., 2009).

Direct measurements of  $^{222}\text{Rn}$  exhalation rates from the soil using the methodology described in Sect. 3.2.2 were performed over a 1-year period, from September 2005 till September 2006. To allow direct comparison with the night-time  $^{222}\text{Rn}$  fluxes derived from measurements of atmospheric  $^{222}\text{Rn}$  content and observations of the mixing layer height, only measurements performed during the days for which sodar-assisted  $^{222}\text{Rn}$  fluxes were available were considered. The monthly mean  $^{222}\text{Rn}$  fluxes derived using both approaches are shown in Fig. 6. The mean  $^{222}\text{Rn}$  flux derived from chamber measurements ( $50.3 \pm 8.4 \text{ Bq m}^{-2} \text{ h}^{-1}$ ) agrees very well with the sodar-assisted estimate of this flux ( $50.3 \pm 3.4 \text{ Bq m}^{-2} \text{ h}^{-1}$ ). A large discrepancy is apparent for February and March 2006, for which the chamber measurements differ from sodar-assisted estimates of the  $^{222}\text{Rn}$  flux by a factor of 10. The reasons for such a large difference remain unclear. It may stem from the fact that frozen soil and snow cover observed at the measurement site in February and the first half of March could partly block the  $^{222}\text{Rn}$  flux from the soil, resulting in low readings of the chamber method, whereas the sodar-assisted estimates of the  $^{222}\text{Rn}$  flux are spatial averages over the footprint area of atmospheric  $^{222}\text{Rn}$  measurements which is of the order of several square kilometres.



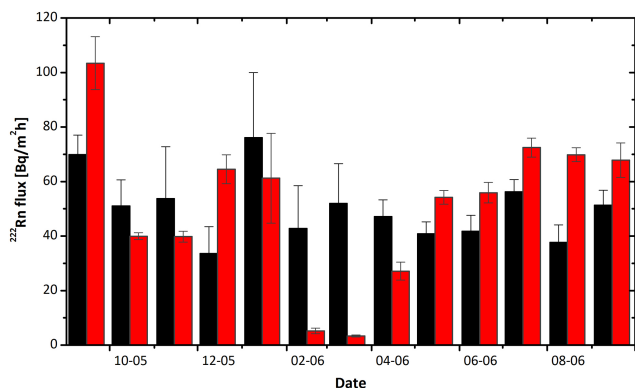


**Figure 6.** Comparison of monthly means of night-time surface fluxes of  $^{222}\text{Rn}$  in Krakow for the period from September 2005 till September 2006, derived from direct measurements of soil  $^{222}\text{Rn}$  flux using the chamber method (red bars) and from atmospheric  $^{222}\text{Rn}$  observations combined with sodar measurements of the mixing layer height (black bars). Error bars indicate standard uncertainty of the mean values.

#### 4.5 Factors controlling seasonality of $^{222}\text{Rn}$ content in the near-ground atmosphere over central Europe

The distinct seasonality of atmospheric  $^{222}\text{Rn}$  concentrations apparent in the data presented in Figs. 1 and 4 may have its roots in several processes: (i) it may reflect seasonal bias in the origin of air masses arriving at the given measurement location, e.g. prevalence of maritime air masses with low  $^{222}\text{Rn}$  during summer and of continental air masses with higher average  $^{222}\text{Rn}$  content during autumn and winter; (ii) it may reflect seasonal bias in the stability of the lower atmosphere, with more frequent, prolonged inversion periods during autumn and winter months as compared to summer; and, finally, (iii) it may reflect seasonality in the source term, i.e. seasonally varying  $^{222}\text{Rn}$  exhalation rates from the soil. All three of these factors may act together, and they are examined in some detail below.

Backward trajectory analysis has been performed for Krakow and Heidelberg for the period from January 2005 till December 2009 using the HYSPLIT (Hybrid Single Particle Lagrangian Integrated Trajectory) model (Draxler and Rolph, 2011). Ninety-six h backward trajectories were calculated for every hour within this time period. Multiple trajectories were displayed by creating an arbitrary grid over the computational domain, counting number of trajectories over each grid point (without multiple intersections of the same trajectory) and dividing it by the total number of trajectories. The plotting routine was used (Rolph, 2011) to display the spatial distribution of trajectory densities over the computational domain. The grid resolution has been set to  $1^\circ \times 1^\circ$ . The results were averaged separately for each season and each site and are presented in Fig. 7. The colour yellow represents grid points where more than 10 % of all

trajectories passed through. The colours blue, green and cyan represent the trajectory density range between 5 and 10 %, 2 and 5 % and 1 and 2 %, respectively. The trajectory density plots shown in Fig. 7 are supplemented by statistical analysis of trajectory height. The distribution of the mean and the maximum trajectory height, separately for each season and each monitoring site, is presented in Fig. S4 in the Supplement. The characteristic feature of these distributions is generally lower height of trajectories arriving in Krakow as compared to Heidelberg. Also, the largest percentage of trajectories arriving in Krakow typically falls into the lowermost range of heights, whereas in Heidelberg distinct maxima of the distributions are observed.

It is apparent from Fig. 7 that only minor seasonal variations occur in the spatial extension and shape of the trajectory density distribution maps for 96 h backward trajectories arriving in Krakow and Heidelberg. The contours are generally skewed towards the W–E axis, reflecting dominance of westerly circulation. There are three distinct differences between Heidelberg and Krakow: (i) Heidelberg receives significantly a higher proportion of maritime air masses originating over the North Atlantic and arriving at the site within 96 h, as when compared to Krakow; (ii) the surface area of the 1 % contour map is larger for Heidelberg than for Krakow, indicating generally higher transport velocities and larger spatial extensions of 96 h backward trajectories for this site; and (iii) the maximum height of trajectories is approximately 3 times higher for Heidelberg as compared to Krakow, indicating transport of air masses being less influenced by surface  $^{222}\text{Rn}$  sources.

In order to better understand the factors controlling the observed seasonality of atmospheric  $^{222}\text{Rn}$  levels at Krakow and Heidelberg, the available data averaged separately for each month and for the entire observation period were compared with other on-site parameters which may influence this apparent seasonality. Figure 8a shows mean monthly distribution of  $^{222}\text{Rn}$  content in the Krakow near-ground atmosphere, presented in the form of a box-and-whisker plot for the entire observation period from January 2005 till December 2009. The long-term monthly mean  $^{222}\text{Rn}$  content shows a broad maximum in the period September–November. The long-term monthly minima of  $^{222}\text{Rn}$ , as observed in Krakow and Heidelberg, are shown in Fig. 8b. Within the quoted uncertainties of the mean values they are indistinguishable at both sites in March, April and May. While the long-term monthly  $^{222}\text{Rn}$  minima are practically constant from March till August in Heidelberg, in Krakow they start to increase already in June. The long-term monthly minima peak in October and November for Heidelberg and Krakow, respectively.

The distinct seasonality observed in atmospheric  $^{222}\text{Rn}$  concentration at both sites could also be linked to the seasonality of  $^{222}\text{Rn}$  emissions from the ground. Monthly mean night-time  $^{222}\text{Rn}$  fluxes, as estimated for Krakow and averaged over the entire observation period (cf. Fig. 5), are shown in Fig. 8c. Figure 8d shows the monthly means of

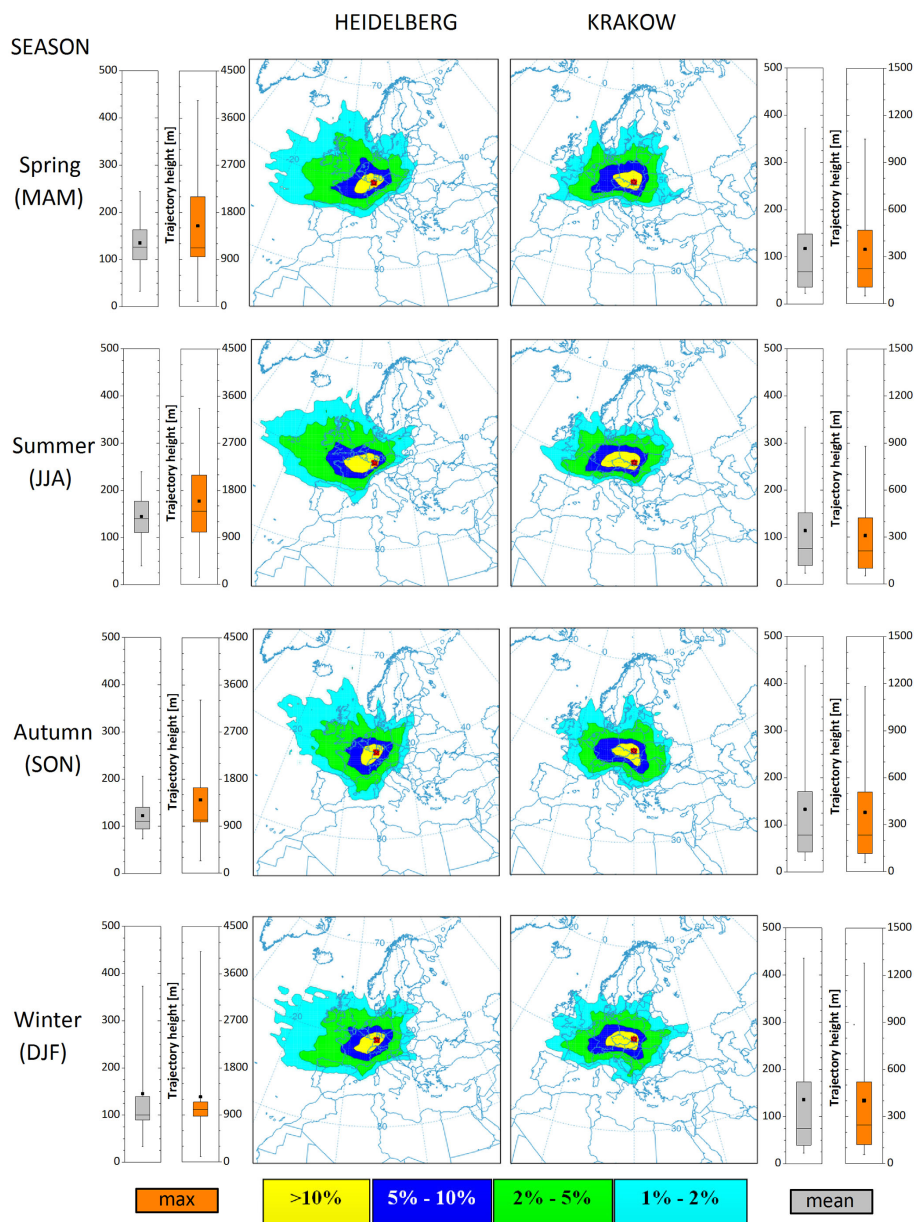


**Figure 7.** Spatial distribution of 96 h backward trajectories of the air masses arriving in Heidelberg, southern Germany, and Krakow, southern Poland, during the period January 2005–December 2009, shown for four seasons, calculated using the HYSPLIT model (Draxler and Rolph, 2011; Rolph, 2011) – see text for details. The maps are supplemented with statistics of trajectory height for each season and station. Marked percentiles represent the 5, 25, 75 and 95 % confidence interval; black squares represent medians; and horizontal lines represent mean values.

$^{222}\text{Rn}$  fluxes derived from chamber measurements performed in Krakow and averaged over the period from September 2005 till September 2006. The monthly night-time  $^{222}\text{Rn}$  fluxes (Fig. 8c) reveal a broad maximum during summer and early autumn (June–October). Although the mean monthly  $^{222}\text{Rn}$  fluxes derived from chamber measurements are more variable, they also reveal a broad maximum during summer and early autumn. Comparison of the amplitudes of seasonal variation presented in Fig. 8a and b with Fig. 8c and d shows that the apparent seasonality in  $^{222}\text{Rn}$  emissions from

the ground cannot fully account for the observed seasonality of the  $^{222}\text{Rn}$  concentrations in the near-ground atmosphere. Also other factors should be involved.

The surface  $^{222}\text{Rn}$  fluxes estimated in the framework of this study reveal distinct seasonality, with a broad maximum during summer and early autumn and minimum during winter. Theoretical considerations (e.g. Nazaroff, 1992; Sasaki et al., 2004) as well as a large body of experimental data (e.g. Rogers and Nielson, 1991; Greeman and Rose, 1996; Levin et al., 2002; Papachristodoulou et al., 2007; Sakoda

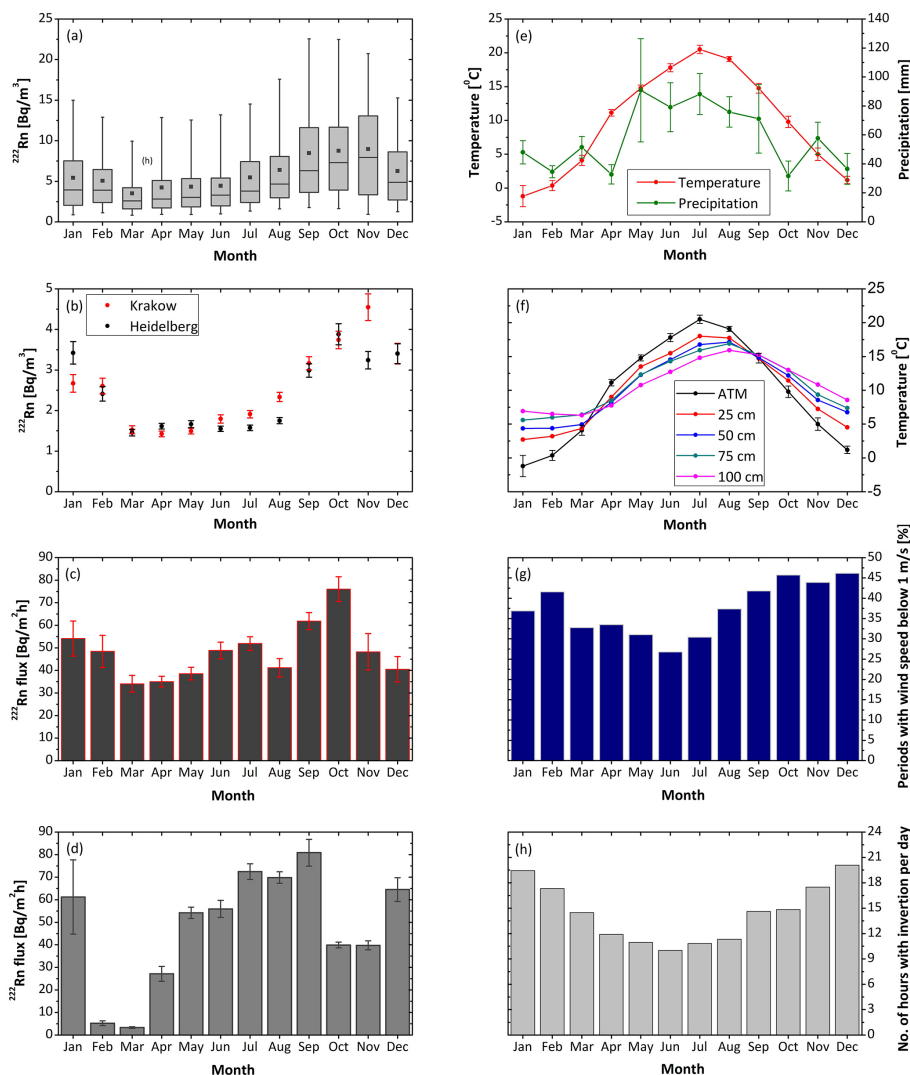


**Figure 8.** (a) Box-and-whisker plot of monthly  $^{222}\text{Rn}$  concentration measured in the near-ground atmosphere of Krakow. The median is represented by horizontal line, while the arithmetic average is shown by a full dot. (b) Monthly minima of atmospheric  $^{222}\text{Rn}$  content, as observed in Krakow and Heidelberg, calculated as arithmetic averages of daily  $^{222}\text{Rn}$  minima for the given month, averaged over the entire observation period from January 2005 till December 2009. (c) Monthly means of night-time  $^{222}\text{Rn}$  fluxes in Krakow, averaged over the period from June 2004 till May 2009. (d) Monthly means of soil  $^{222}\text{Rn}$  fluxes in Krakow derived from chamber measurements, averaged over the period from September 2005 till September 2006. (e) Monthly means of surface air temperature and precipitation in Krakow, averaged over the period from January 2005 till December 2009. (f) Monthly means of surface air and soil temperatures in Krakow. (g) Percentage of periods with wind speed below  $1\text{ m s}^{-1}$  in Krakow, averaged over the period from January 2005 till December 2009. (h) Monthly means of number of hours with ground-based inversion per day, averaged over the period from January 1994 till December 1999.

et al., 2010) suggest that free pore space in the soil available for diffusion-controlled transport of gaseous  $^{222}\text{Rn}$  exerts primary control over  $^{222}\text{Rn}$  exhalation rates. This parameter can be approximated by the volumetric water content in the soil profile. The maps of soil moisture available for the European continent (<http://edo.jrc.ec.europa.eu>) reveal generally lower values of this parameter during summer and autumn as compared to winter and spring, for large parts of continental Europe. This suggests that the distinct seasonality of  $^{222}\text{Rn}$

exhalation rates, as observed in this study, may have its origin in seasonal changes of moisture load in the upper soil level.

Monthly means of surface air temperature and the amounts of monthly precipitation, both recorded in Krakow and averaged over the period from January 2005 till December 2009, are shown in Fig. 8e. While the air temperature reveals distinct seasonal changes (the difference between the coldest and warmest month is larger than  $20\text{ }^{\circ}\text{C}$ ), monthly precipitation data are more variable and the seasonality is less marked. Comparison of local air and soil temperatures (four different

depths) in the vicinity of  $^{222}\text{Rn}$  concentration measurements in Krakow is shown in Fig. 8f. As seen in Fig. 8f, during autumn and winter the soil is warmer than air, thus making the soil air unstable. This may facilitate transport of  $^{222}\text{Rn}$  from the soil to the atmosphere (Schubert and Schulz, 2002).

The last two graphs in Fig. 8g and h show seasonal variations of two parameters characterizing stability of the lower atmosphere in Krakow: (i) the wind speed and (ii) the duration of inversion episodes. In Fig. 8g monthly means of the percentage of calm periods (wind speed below  $1\text{ m s}^{-1}$ ), averaged over the entire observation period (January 2005–December 2009), are shown. It is apparent that the percentage of periods with wind speed below  $1\text{ m s}^{-1}$  is highest in Krakow during autumn and winter. Also, the duration of the inversion periods is highest during that time (October–February), contributing to enhanced stability of the lower atmosphere. Although the data presented in Fig. 8h refer to another 5-year period (January 1994–December 1999), it is assumed that this specific feature of the local atmosphere in Krakow, when averaged over a 5-year period, is valid also for the period considered in this study (January 2005–December 2009).

#### 4.6 Assessment of $^{222}\text{Rn}$ build-up in the atmosphere over the European continent

Fluxes of  $^{222}\text{Rn}$  over the ocean are 2 to 3 orders of magnitude smaller than those over the continents (Schery and Huang, 2004). Consequently, maritime air masses entering the continent will have very low  $^{222}\text{Rn}$  content and will be gradually laden with  $^{222}\text{Rn}$  until new equilibrium is reached. Since both  $^{222}\text{Rn}$  observation sites discussed in this study are located in the same latitudinal band (ca.  $50^\circ\text{ N}$ ) and are exposed to westerly circulation, with Heidelberg being situated ca. 600 km from the Atlantic coast and Krakow approximately 1000 km further inland, it was of interest to quantify the extent of  $^{222}\text{Rn}$  build-up in the air masses on their way from Heidelberg to Krakow. The evolution of  $^{222}\text{Rn}$  content within the PBL can be described by a simple mass balance equation:

$$\frac{dC_{\text{Rn}}}{dt} = S_{\text{Rn}} - (\lambda_{\text{d}} + \lambda_{\text{e}})C_{\text{Rn}}, \quad (5)$$

where  $C_{\text{Rn}}$  is the concentration of  $^{222}\text{Rn}$  in the convective mixed layer of the PBL and  $S_{\text{Rn}}$  is the source term linked to the surface flux of  $^{222}\text{Rn}$ .  $S_{\text{Rn}} = F_{\text{Rn}}/h$ , where  $F_{\text{Rn}}$  is the surface flux of  $^{222}\text{Rn}$  and  $h$  is the height of the convective mixed layer;  $\lambda_{\text{d}}$  is the decay constant of  $^{222}\text{Rn}$ ; and  $\lambda_{\text{e}}$  is rate constant associated with removal of  $^{222}\text{Rn}$  across the PBL boundary. Equation (5) implies perfect mixing within the PBL and assumes that net exchange of  $^{222}\text{Rn}$  due to horizontal transport perpendicular to the direction of air mass movement is equal to 0. It has to be noted that convective mixed layer referred to in Eq. (5) extends to the PBL boundary, while the nocturnal mixing layer discussed in Sect. 3.2.1

is generally less extensive ( $H < h$ ) and occupies only part of the PBL (Stull, 1988). Analytical solution of Eq. (5) – with the initial condition  $C_{\text{Rn}}(0) = 0$ , constant surface flux of  $^{222}\text{Rn}$  and constant height of the convective mixed layer – reads as follows:

$$C_{\text{Rn}}(t) = \frac{S_{\text{Rn}}}{\lambda_{\text{d}} + \lambda_{\text{e}}} \left( 1 - e^{-(\lambda_{\text{d}} + \lambda_{\text{e}})t} \right). \quad (6)$$

Substituting  $S_{\text{Rn}} = F_{\text{Rn}}/h$  and  $T_{\text{eff}} = 0.693/(\lambda_{\text{d}} + \lambda_{\text{e}})$ ,

$$C_{\text{Rn}}(t) = \frac{F_{\text{Rn}} \cdot T_{\text{eff}}}{h \cdot 0.693} \left( 1 - e^{-\frac{0.693}{T_{\text{eff}}}t} \right). \quad (7)$$

Equation (7) can be used to calculate the expected build-up of  $^{222}\text{Rn}$  content within the PBL for maritime air masses travelling eastward from the Atlantic Ocean towards Heidelberg and Krakow. It is apparent from the preceding discussion that local effects are decisive in shaping up atmospheric  $^{222}\text{Rn}$  levels at both sites. Therefore, careful screening and selection of  $^{222}\text{Rn}$  data had to be performed before an attempt was made to quantify the continental effect between both sites.

In the first step, only trajectories arriving in Krakow which also passed Heidelberg at the distance of less than 100 km were selected for further analysis (Fig. 9). Out of this population of trajectories, only those which were travelling from the vicinity of Heidelberg to Krakow during the period shorter than 24 h, were selected. Finally, only the data representing minimum  $^{222}\text{Rn}$  concentrations measured at both sites during these periods, taking into account the time lag due to atmospheric transport from Heidelberg to Krakow, were considered. This step was aimed at minimizing the impact of local effects (inversion episodes) on the measured  $^{222}\text{Rn}$  concentrations at both sites. The selected minimum  $^{222}\text{Rn}$  concentrations (94 pairs), averaged over the entire observation period (January 2005–December 2009) separately for each station, are equal to  $1.12 \pm 0.09$  and  $1.90 \pm 0.11\text{ Bq m}^{-3}$  for Heidelberg and Krakow, respectively. The difference ( $0.78 \pm 0.12\text{ Bq m}^{-3}$ ) represents mean build-up of  $^{222}\text{Rn}$  content between Heidelberg and Krakow.

Sensitivity analysis of Eq. (7) was made with an attempt to fit simultaneously three values: the measured mean minimum  $^{222}\text{Rn}$  concentrations at (i) Heidelberg and (ii) Krakow, and (iii) the difference between them. Three parameters in Eq. (7) were treated as adjustable parameters: (i) the mean transport velocity ( $V$ ) of the air masses within the convective mixed layer of the PBL, on their route from the Atlantic coast to Heidelberg and Krakow; (ii) the mean surface flux of  $^{222}\text{Rn}$  ( $F_{\text{Rn}}$ ) on the European continent from the Atlantic coast till Krakow; and (iii) the rate constant of  $^{222}\text{Rn}$  removal across the top of the PBL ( $\lambda_{\text{e}}$ ). Since HYSPLIT routinely returns also the mixing height of the calculated backward trajectories, it was possible to derive the value of this parameter directly from the model output. The mixing heights were calculated for all trajectories which satisfied the selection criteria outlined above, and the maximum mixing height

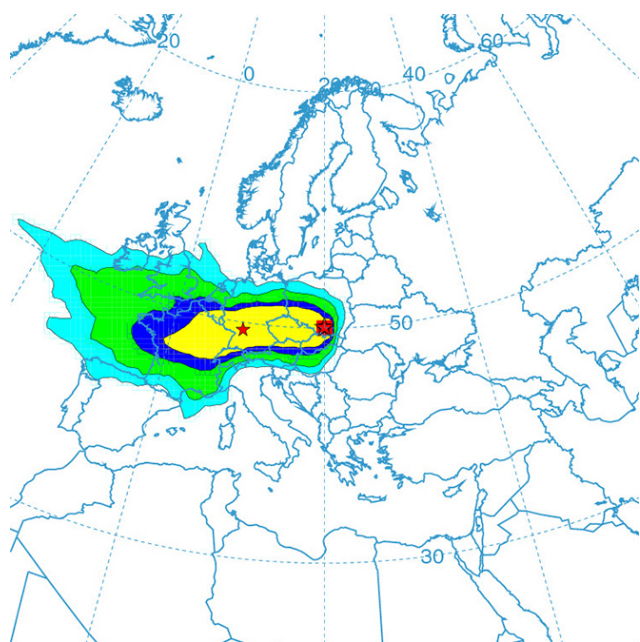


**Figure 9.** Spatial distribution of 96 h backward trajectories of the air masses arriving in Krakow, southern Poland, which passed Heidelberg, southern Germany, at the distance of less than 100 km, calculated using the HYSPLIT model (Draxler and Rolph, 2011; Rolph, 2011 – see text for details). The analysis comprised the period from January 2005 till December 2009.

for each trajectory was selected. Averaged over all trajectories considered in the calculation, this procedure yields the mean value of the convective mixed layer height equal to  $1083 \pm 31$  m. In calculations 1100 m was adopted. The selection of 94 h trajectories imposes a lower limit on the velocity of air masses travelling from the Atlantic coast to Heidelberg and Krakow, equal to approximately  $2.8 \text{ m s}^{-1}$ . The values of transport velocities used in sensitivity analysis varied between  $3.0$  and  $4.0 \text{ m s}^{-1}$ . It appeared that, while the calculated  $^{222}\text{Rn}$  concentrations at Heidelberg and Krakow depend on the assumed transport velocity, the difference between them is relatively insensitive to the actual value of this parameter. The rate constant of radon removal across the top of the PBL ( $\lambda_e$ ) and the mean surface  $^{222}\text{Rn}$  flux varied in the calculations from  $\lambda_e = 0.5\lambda_d$  to  $\lambda_e = 1.5\lambda_d$  and from  $30$  to  $60 \text{ Bq m}^{-2} \text{ h}^{-1}$ , respectively.

Goodness of the fitting procedure was quantified by calculating the sum of squared differences ( $\Sigma(C_{\text{Rn}(m)} - C_{\text{Rn}(c)})^2$ ) between the measured ( $C_{\text{Rn}(m)}$ ) and calculated ( $C_{\text{Rn}(c)}$ ) mean minimum  $^{222}\text{Rn}$  concentration at Heidelberg and Krakow, and the difference between them. The best fit ( $\Sigma = 9.9 \times 10^{-4}$ ) was obtained for the following combination of the adjusted parameters:  $V = 3.5 \text{ m s}^{-1}$ ,  $F_{\text{Rn}} = 36 \text{ Bq m}^{-2} \text{ h}^{-1}$  and  $\lambda_e = \lambda_d$ . Similarity between the rate constant of radon removal across the top of the PBL and the decay constant of  $^{222}\text{Rn}$  was suggested also by Lui et al. (1984). The

mean continental  $^{222}\text{Rn}$  surface flux between the Atlantic coast and Krakow obtained through the fitting procedure ( $36 \text{ Bq m}^{-2} \text{ h}^{-1}$ ) is lower than the mean annual  $^{222}\text{Rn}$  flux obtained for the Krakow urban area in the framework of this study (ca.  $47 \text{ Bq m}^{-2} \text{ h}^{-1}$ ) and is significantly lower than the annual mean  $^{222}\text{Rn}$  flux (ca.  $57 \text{ Bq m}^{-2} \text{ h}^{-1}$ ) estimated for the Heidelberg area from long-term flux measurements at five locations with different soil texture (Schmidt et al., 2003). If the mean surface  $^{222}\text{Rn}$  flux of  $52 \text{ Bq m}^{-2} \text{ h}^{-1}$  is assumed (arithmetic average of Heidelberg and Krakow best estimates of this parameter), an equally good fit of the measured minimum  $^{222}\text{Rn}$  concentrations at both stations and the difference between them is also possible, albeit with a significantly larger height of the convective mixed layer ( $h = 1600$  m). This suggests that the modelled value of the convective mixing layer is underestimated.

## 5 Conclusions

Systematic observations of  $^{222}\text{Rn}$  concentration in the near-ground atmosphere at two continental sites in Europe, supplemented by measurements of surface  $^{222}\text{Rn}$  fluxes, allowed a deeper insight into factors controlling spatial and temporal variability of  $^{222}\text{Rn}$  in the near-ground atmosphere over central Europe. The available data allowed us to address the role of local and regional factors in controlling the observed atmospheric  $^{222}\text{Rn}$  levels and their variability.

Atmospheric concentrations of  $^{222}\text{Rn}$  at both observation sites vary on daily, synoptic and monthly timescales. Generally higher and more variable  $^{222}\text{Rn}$  concentrations recorded in Krakow are mainly due to specific characteristics of the local atmosphere, such as lower wind speed and more frequent inversion periods of prolonged duration as compared to Heidelberg, thus leading to enhanced stability of the lower atmosphere at this monitoring site.

The presented data reveal a distinct asymmetry in the shape of seasonal variations of surface  $^{222}\text{Rn}$  fluxes and  $^{222}\text{Rn}$  concentrations measured in the local atmosphere of Krakow. While atmospheric  $^{222}\text{Rn}$  contents peak in November, the  $^{222}\text{Rn}$  exhalation rates reach their maximum in September–October. This distinct phase shift stems most probably from increased stability of the lower atmosphere during autumn months (higher percentage of still periods, longer duration of ground-based inversion episodes). These factors may collectively lead to the observed  $^{222}\text{Rn}$  maximum in the local atmosphere in November, despite already-weakening soil  $^{222}\text{Rn}$  flux at that time of the year.

Although the atmospheric  $^{222}\text{Rn}$  levels at Heidelberg and Krakow appeared to be controlled primarily by local factors, it was nevertheless possible to evaluate the continental effect in atmospheric  $^{222}\text{Rn}$  content between both sites, related to gradual build-up of  $^{222}\text{Rn}$  load of maritime air masses travelling eastward over the European continent. Satisfactory agreement obtained between the measured and modelled

minimum  $^{222}\text{Rn}$  concentrations at both sites and the difference between them, derived from a simple box model coupled with HYSPLIT analysis of air mass trajectories, allowed putting some constraints on the parameters of atmospheric  $^{222}\text{Rn}$  transport over the European continent and its surface fluxes.

**The Supplement related to this article is available online at doi:10.5194/acp-14-9567-2014-supplement.**

*Acknowledgements.* The authors would like to thank Ingeborg Levin from the Institute of Environmental Physics, University of Heidelberg, for providing the radon monitor and the experimental data for Heidelberg, as well as for thoughtful comments on the early version of the manuscript. Thorough reviews of two anonymous referees greatly improved the quality of the manuscript. The work has been partially supported by EU projects EUROHYDROS and CARBOUEROPE, grants of the Ministry of Science and Higher Education (project nos. 2256/B/P01/2007/33 and 4132/B/T02/2008/43) and the statutory funds of the AGH University of Science and Technology (project no. 11.11.220.01). The authors gratefully acknowledge the NOAA Air Resources Laboratory (ARL) for the provision of the HYSPLIT transport and dispersion model and READY website (<http://www.arl.noaa.gov/ready.php>) used in this publication.

Edited by: E. Gerasopoulos

## References

- Bergamaschi, P., Meirink, J. F., Müller, J. F., Körner, S., Heimann, M., Dlugokencky, E. J., Kaminski, U., Marcaccian, G., Vecchi, R., Meinhardt, F., Ramonet, M., Sartorius, H., and Zahorowski, W.: Model Inter-comparison on Transport and Chemistry – Report on Model Inter-comparison Performed Within European Commission FP5 Project EVERGREEN (“Global Satellite Observation of Greenhouse Gas Emissions”). European Commission, DG Joint Research Centre, Institute for Environment and Sustainability, p. 53, 2006
- Biraud, S., Ciais, P., Ramonet, M., Simmonds, P., Kazan, V., Monfray, P., O’Doherty, S., Spain, T. G., and Jennings, S. G.: European greenhouse gas emissions estimated from continuous atmospheric measurements and radon 222 at Mace Head, Ireland, *J. Geophys. Res.*, 105, 1351–1366, 2000.
- Chevillard, A., Ciais, P., Karstens, U., Heimann, M., Schmidt, M., Levin, I., Jacob, D., Podzun, R., Kazan, V., Sartorius, H., and Weingartner, E.: Transport of  $^{222}\text{Rn}$  using the regional model REMO: a detailed comparison with measurements over Europe, *Tellus B*, 54, 850–871, 2002.
- Conen, F., Neftel, A., Schmid, M., and Lehmann, B. E.:  $\text{N}_2\text{O}/^{222}\text{Rn}$ -soil flux calibration in the stable nocturnal surface layer, *Geophys. Res. Lett.*, 29, 1025, doi:10.1029/2001GL013429, 2002.
- Dörr, H., Kromer, B., Levin, I., Münnich, K. O., and Volpp, J.-J.:  $\text{CO}_2$  and  $^{222}\text{Rn}$  as tracers for atmospheric transport, *J. Geophys. Res.*, 88, 1309–1313, 1983.
- Draxler, R. R. and Rolph, G. D.: HYSPLIT (HYbrid Single-Particle Lagrangian Integrated Trajectory) Model access via NOAA ARL READY Website (<http://ready.arl.noaa.gov/HYSPLIT.php>). NOAA Air Resources Laboratory, Silver Spring, MD, 2011.
- Gerasopoulos, E., Kouvarakis, G., Vrekoussis, M., Kanakidou, M., and Mihalopoulos N.: Ozone variability in the marine boundary layer of the eastern Mediterranean based on 7-year observations, *J. Geophys. Res.*, 110, D15309, doi:10.1029/2005JD005991, 2005.
- Greeman, D. J. and Rose, A. W.: Factors controlling the emanation of radon and thoron in soils of the eastern USA, *Chem. Geol.*, 129, 1–14, 1996.
- Gupta, M., Douglass, A. R., Kawa, S., and Pawson, S.: Use of radon for evaluation of atmospheric transport models: sensitivity to emissions, *Tellus B*, 56, 404–412, 2004.
- IUSS Working Group WRB, World Reference Base for Soil Resources 2006, First Update 2007, World Soil Resources Reports 103, Food and Agriculture Organization, Rome, 118 pp., 2007.
- Jacob, D., Prather, M., Rasch, P., Shia, R., Balkanski, Y., Beagley, S., Bergmann, D., Blackshear, W., Brown, M., Chiba, M., Chipperfield M., de Grandpre, J., Dignon, J., Feichter, J., Genthon, C., Grose, W., Kasibhatla, P., Kohler, I., Kritz, M., Law, K., Penner, J., Ramonet, M., Reeves, C., Rotman, D., Stockwell, D., Van Velthoven, P., Verver, G., Wild, O., Yang, H., and Zimmermann, P.: Evaluation and intercomparison of global atmospheric transport models using  $^{222}\text{Rn}$  and other short-lived tracers, *J. Geophys. Res.*, 102, 5953–5970, 1997.
- Jeričević, A., Kraljević, L., Grisogono, B., Fagerli, H., and Večenaj, Ž.: Parameterization of vertical diffusion and the atmospheric boundary layer height determination in the EMEP model, *Atmos. Chem. Phys.*, 10, 341–364, doi:10.5194/acp-10-341-2010, 2010.
- Levin, I., Glatzel-Mattheier, H., Marik, T., Cuntz, M., and Schmidt, M.: Verification of German methane emission inventories and their recent changes based on atmospheric observations. *J. Geophys. Res.*, 104, 3447–3456, 1999.
- Levin, I., Born, M., Cuntz, M., Langendörfer, U., Mantsch, S., Naegler, T., Schmidt, M., Varlagin, A., Verclas, S., and Vagenbach, D.: Observations of atmospheric variability and soil exhalation rate of radon-222 at a Russian forest site, *Tellus B*, 54, 462–475, 2002.
- Levin, I., Kromer, B., Schmidt, M., and Sartorius, H.: A novel approach for independent budgeting of fossil fuel  $\text{CO}_2$  over Europe by  $^{14}\text{CO}_2$  observations, *Geophys. Res. Lett.*, 30, 2194, doi:10.1029/2003GL018477, 2003.
- Lui, S. C., McAfee, J. R., and Cicerone, R. J.: Radon 222 and tropospheric vertical transport, *J. Geophys. Res.*, 89, 7291–7297, 1984.
- Mazur, J.: Dynamics of radon exhalation rates in relation to meteorological parameters and properties of soil. PhD Thesis, Henryk Niewodniczanski Institute of Nuclear Physics, Polish Academy of Science, Krakow, 140 pp., [www.ifj.edu.pl/publ/reports/2008\\_2008](http://www.ifj.edu.pl/publ/reports/2008_2008) (in Polish).
- Nazaroff, W.: Radon transport from soil to air, *Rev. Geophys.*, 30, 137–160, 1992.
- Netzel, P., Stano, S., and Zarebski, M.: Vertical doppler sodar VDS, *Wiad. IMGW*, 18, 119–125, 1995.
- Papachristodoulou, C., Ioannides, K., and Spathis, S.: The effect of moisture content on radon diffusion through soil: assessment

- in laboratory and field experiments, *Health Phys.*, 92, 257–264, 2007.
- Piringer, M. and Joffre, S. (Ed.): *The Urban Surface Energy Budget and Mixing Height in European Cities: Data, Models and Challenges for Urban Meteorology and Air Quality*, Final Report of Working Group 2 of COST-715 Action, Demetra Ltd Publishers, Bulgaria, 2005.
- Rogers, V. C. and Nielson, K. K.: Correlations for predicting air permeabilities and  $^{222}\text{Rn}$  diffusion coefficients of soils, *Health Phys.*, 61, 225–230, 1991.
- Rolph, G. D.: Real-time Environmental Application and Display sYstem (READY) Website (<http://ready.arl.noaa.gov>). NOAA Air Resources Laboratory, Silver Spring, MD, 2011.
- Sakoda, A., Ishimori, Y., Hanamoto, K., Kataoka, T., Kawabe, A., and Yamaoka, K.: Experimental and modeling studies of grain size and moisture content effects on radon emanation, *Radiat. Meas.*, 45, 204–210, 2010.
- Sasaki, T., Gunji, Y., and Okuda, T.: Mathematical modelling of Radon emanation, *J. Nucl. Sci. Tech.*, 41, 142–151, 2004.
- Schery, S. D. and Huang, S.: An estimate of the global distribution of radon emissions from the ocean, *Geophys. Res. Lett.*, 31, L19104, doi:10.1029/2004GL021051, 2004.
- Schmidt, M., Graul, R., Sartorius, H., and Levin, I.: Carbon dioxide and methane in continental Europe: a climatology, and  $^{222}\text{Rn}$ -based emission estimates, *Tellus B*, 48, 457–473, 1996.
- Schmidt, M., Graul, R., Sartorius, H., and Levin, I.: The Schauinsland  $\text{CO}_2$  record: 30 years of continental observations and their implications for the variability of the European  $\text{CO}_2$  budget, *J. Geophys. Res.*, 108, 4619, doi:10.1029/2002JD003085, 2003.
- Schubert, M. and Schulz, H.: Diurnal radon variations in the upper soil layers and at the soil-air interface related to meteorological parameters, *Health Phys.*, 83, 91–96, 2002.
- Servant, J. and Tanaevsky, O.: Mesures de la radioactivite naturelle dans la region Parisienne, *Ann. Geophys.*, 17, 405–409, 1961, <http://www.ann-geophys.net/17/405/1961/>.
- Simpson, D., Benedictow, A., Berge, H., Bergström, R., Emberson, L. D., Fagerli, H., Flechard, C. R., Hayman, G. D., Gauss, M., Jonson, J. E., Jenkin, M. E., Nyíri, A., Richter, C., Semeena, V. S., Tsyro, S., Tuovinen, J.-P., Valdebenito, Á., and Wind, P.: The EMEP MSC-W chemical transport model – technical description, *Atmos. Chem. Phys.*, 12, 7825–7865, doi:10.5194/acp-12-7825-2012, 2012.
- Stull, R. B.: *An introduction to boundary layer meteorology*, Reidel Publishing Co., Dordrecht, 666 pp., 1988.
- Szegvary, T., Conen, F., and Ciais, P.: European  $^{222}\text{Rn}$  inventory for applied atmospheric studies, *Atmos. Environ.*, 43, 1536–1539, 2009.
- Taguchi, S., Law, R. M., Rödenbeck, C., Patra, P. K., Maksyutov, S., Zaborowski, W., Sartorius, H., and Levin, I.: TransCom continuous experiment: comparison of  $^{222}\text{Rn}$  transport at hourly time scales at three stations in Germany, *Atmos. Chem. Phys.*, 11, 10071–10084, doi:10.5194/acp-11-10071-2011, 2011.
- Thoning, K. W., Tans, P. P., and Komhyr, W. D.: Atmospheric carbon dioxide at Mauna Loa Observatory 2. Analysis of the NOAA GMCC data, 1974–1985, *J. Geophys. Res.*, 94, 8549–8565, 1989.
- van der Laan, S., Neubert, R. E. M., and Meijer, H. A. J.: Methane and nitrous oxide emissions in The Netherlands: ambient measurements support the national inventories, *Atmos. Chem. Phys.*, 9, 9369–9379, doi:10.5194/acp-9-9369-2009, 2009.
- van der Laan, S., Karstens, U., Neubert, R. E. M., Van der Laan-Luijckx, I. T., and Meijer, H. A. J.: Observation-based estimates of fossil fuel-derived  $\text{CO}_2$  emissions in the Netherlands using  $\Delta^{14}\text{C}$ ,  $\text{CO}$  and  $^{222}\text{Rn}$ , *Tellus B*, 62, 89–402, 2010.
- Vaupotič, J., Gregorič, A., Kobal, I., Žvab, P., Kozak, K., Mazur, J., Kochowska, E., and Grządziel, D.: Radon concentration in soil gas and radon exhalation rate at the Ravne Fault in NW Slovenia, *Nat. Hazards Earth Syst. Sci.*, 10, 895–899, doi:10.5194/nhess-10-895-2010, 2010.
- Wigand A. and Wenk F.: Air composition and Radium emanation from measurements during plane take-off, *Annalen der Physik*, 86, 657–686, 1928 (in German).
- Williams, A. G., Zaborowski, W., Chambers, S., Hacker, J. M., Schelander, P., Element, A., Werczynski, S., and Griffiths, A.: Mixing and venting in clear and cloudy boundary layers using airborne radon measurements, American Meteorological Society's 18th Symposium on Boundary Layers and Turbulence, 9–13 June 2008, Stockholm, Sweden, 2008.
- Wilson, S. R., Dick, A. L., Fraser, P. J., and Whittlestone, S.: Nitrous oxide flux estimates from south-east Australia, *J. Atmos. Chem.*, 26, 169–188, 1997.
- Zaborowski, W., Williams, A. G., Vermeulen, A. T., Chambers, S., Crawford, J., and Sisouham, O.: Diurnal Boundary Layer Mixing Patterns Characterised by Radon-222 Gradient Observations at Cabauw, American Meteorological Society's 18th Symposium on Boundary Layers and Turbulence, 9–13 June 2008, Stockholm, Sweden, 2008.
- Zaborowski, W., Chambers, S., Crawford, J., Williams, A. G., Cohen, D. D., Vermeulen, A. T., and Verheggen, B.:  $^{222}\text{Rn}$  Observations for Climate and Air Quality Studies. Sources and Measurements of Radon and Radon Progeny Applied to Climate and Air Quality Studies, Proceedings of a Technical Meeting, IAEA, Vienna, Austria, 77–96, 2011.
- Zhang, K., Wan, H., Zhang, M., and Wang, B.: Evaluation of the atmospheric transport in a GCM using radon measurements: sensitivity to cumulus convection parameterization, *Atmos. Chem. Phys.*, 8, 2811–2832, doi:10.5194/acp-8-2811-2008, 2008.
- Zhang, K., Feichter, J., Kazil, J., Wan, H., Zhuo, W., Griffiths, A. D., Sartorius, H., Zaborowski, W., Ramonet, M., Schmidt, M., Yver, C., Neubert, R. E. M., and Brunke, E.-G.: Radon activity in the lower troposphere and its impact on ionization rate: a global estimate using different radon emissions, *Atmos. Chem. Phys.*, 11, 7817–7838, doi:10.5194/acp-11-7817-2011, 2011.
- Zimnoch, M., Godłowska, J., Necki, J. M., and Rozanski, K.: Assessing surface fluxes of  $\text{CO}_2$  and  $\text{CH}_4$  in urban environment: a reconnaissance study in Krakow, Southern Poland, *Tellus B*, 62, 573–580, 2010.